

Nonergodicity and light scattering from polymer gels

J.-Z. Xue

*Exxon Research and Engineering Company, Route 22 East, Annandale, New Jersey 08801
and Department of Physics, Princeton University, Princeton, New Jersey 08540*

D. J. Pine and S. T. Milner

Exxon Research and Engineering Company, Route 22 East, Annandale, New Jersey 08801

X.-l. Wu

Department of Physics, University of Pittsburgh, Pittsburgh, Pennsylvania 15260

P. M. Chaikin

*Exxon Research and Engineering Company, Route 22 East, Annandale, New Jersey 08801
and Department of Physics, Princeton University, Princeton, New Jersey 08540*

(Received 10 March 1992)

Dynamic light scattering from polymer gels is complicated by the fact that the scattering intensity and its time correlation function change as different parts of a sample are explored. This results from the nonergodicity of the sample—time averages are not the same as ensemble averages, the result of a finite rigidity that leads to constrained inhomogeneities. We demonstrate a direct technique for ensemble averaging (by moving the sample), present the experimental correlation function containing correlations that do not decay with time, and show that the light scattering results from a superposition of static scattering from immobile inhomogeneities and dynamic density fluctuations from “gel modes.”

PACS number(s): 82.70.Gg, 05.40.+j

I. INTRODUCTION

Polymer gel systems are interesting candidates for dynamic-light-scattering (DLS) studies from a number of different viewpoints. The physical properties of the gel, its elasticity, permeability, dangling ends, diffusion of connected and unconnected strands and foreign particles produce readily measurable effects on the density fluctuations which are probed by light scattering [1–4]. However, even casual observation of a polymer gel with ambient light or laser illumination quickly reveals a strong static component of the scattering. Time-independent inhomogeneities are clear to the eye, or in the speckle pattern of light scattered onto nearby surfaces. These static inhomogeneities can lead to long-time correlations which do not decay. This complicates the interpretation of the dynamic-light-scattering data, especially since most commercial correlators are designed to handle systems where the correlation function decays to zero at sufficiently long time. In the polymer gel system there are infinite time correlations which may or may not be of interest to the researcher, but are certainly present and can lead to erroneous interpretations of the data if not treated properly.

On the other hand, the presence of the static inhomogeneities which result from fluctuations during the gelation process give us an interesting opportunity to study the differences between time averages and ensemble averages (different manifestations of the same physical system) in a system where both averages are accessible. Statistical mechanics rests heavily on the assumption that

the ensemble average (which is what we know how to calculate) is the same as the time average (which is what we usually measure) [5].

The problem of dynamic light scattering from polymer gels has been addressed many times before [1, 2, 6, 7]. In many of these experiments the question of the non-ergodicity was not addressed at all. It is surprising that it was possible to obtain any useful information from conventional data since placing the same sample in the same apparatus in different orientations would result in different measured correlation functions. Nevertheless, the experiments were reported and interpreted. There have arisen two models to describe the dynamics and, in some cases, the presence of the static background. In one model the gel is viewed as an elastic medium with overdamped modes describing the density fluctuations [1]. Coupled with some static scattering (or dirt) this picture can qualitatively describe the initial decay of the correlation function and its saturation at long time [6]. A qualitatively similar correlation function is obtained by a model of harmonically bound Brownian particles [7]. At short time the particles undergo simple diffusion, but at longer time they find that they are restricted to a maximum displacement when the elastic energy equals the thermal energy ($k\langle x^2 \rangle / 2 = k_B T / 2$). After correctly ensemble averaging, we find that the distinction between these two proposed behaviors lies in the wave vector or q dependence of their correlation functions. For our polyacrylamide gels, the data are consistent with the model

of gel modes plus static randomly distributed small inhomogeneities and not with the model of harmonically bound Brownian particles.

The question of nonergodicity in relation to DLS experiments and particularly to polymer gels has been previously addressed by Pusey and van Megen [8] and Joosten *et al.* [9]. These authors have found a clever way to obtain the ensemble average correlation function from the time average at a single orientation by comparing the time-average intensity with the ensemble-average intensity. Basically they show that if you find a configuration where the time-average intensity is the ensemble-average intensity, then the time-varying part of the measured correlation function is the same as the time-varying part of the ensemble-averaged correlation function. In this paper, we present an alternative scheme for directly obtaining the correct ensemble-averaged correlation function. Though less clever, our scheme is more robust. Furthermore, the clever technique only works when the intensity of scattered light is detected from an area less than a laser speckle size on the photon detector, only for single scattering, and only if there is *a priori* knowledge that there are no long-time dynamics in the system. Our scheme does not suffer from these limitations. The photon-counting statistics for the two measurement schemes are essentially the same.

II. LASER SPECKLE, TIME AND ENSEMBLE AVERAGES, CORRELATION FUNCTIONS, AND CORRELATORS

In order to illustrate the problems of dynamic light scattering on a nonergodic system it is instructive to return to the elementary concepts of light scattering to look at time and position averages and their fluctuations. In Fig. 1 we show a schematic of the scattering geometry with a coherent beam scattering from a sample and the interference or speckle pattern that it would produce on a screen. The electric field at a point \mathbf{r}_s on the screen is determined by the angle that the scattering vector \mathbf{q} subtends to arrive at that point:

$$\begin{aligned} \mathbf{q} &= \mathbf{k}' - \mathbf{k}, \mathbf{r}_s \approx \mathbf{q}l/\pi, \\ \mathbf{E}(\mathbf{r}_s) &= \sum_j e^{i\mathbf{q}\cdot\mathbf{r}_j}, \end{aligned} \quad (2.1)$$

$$I(\mathbf{r}_s) = \sum_{j,j'} e^{i\mathbf{q}\cdot(\mathbf{r}_j - \mathbf{r}_{j'})} = \sum_{j=j'} 1 + \sum_{j \neq j'} e^{i\mathbf{q}\cdot(\mathbf{r}_j - \mathbf{r}_{j'})},$$

$$\langle I(\mathbf{r}_s) \rangle \pm \langle \delta I \rangle_{\text{rms}} \approx N \pm \sqrt{N^2},$$

where l is the distance to the screen, \mathbf{r}_j is the position of the j th scatterer, and N is the number of scatterers. We have for the moment assumed that nothing is moving and that the scatterers are randomly distributed over a volume that is much larger than the cube of the wavelength of the light. The decomposition of the sum yields two terms. The N interferences from the same scatterers ($j = j'$) give the average value. The N^2 interferences from dissimilar scatterers correspond to a random walk of N^2 steps in complex space. The average is zero but

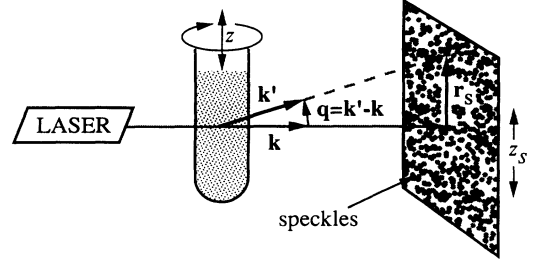


FIG. 1. Schematic geometry for a dynamic-light-scattering experiment, where we imagine that either the sample (coordinates z) or the detector (coordinates z_s) can be translated. The detector is schematically replaced by a screen to illustrate the speckle pattern.

the rms fluctuations are the same magnitude as the mean value. Thus the intensity varies on the screen from zero to about twice its average. A direct calculation gives the distribution of intensities and the value of the fluctuations as [10]

$$P(I) = \frac{e^{-I/\langle I \rangle}}{\langle I \rangle}, \quad \frac{\langle \delta I^2 \rangle}{\langle I \rangle^2} = \frac{\langle I^2 \rangle - \langle I \rangle^2}{\langle I \rangle^2} = 1. \quad (2.2)$$

The intensity fluctuations on the screen are laser speckles. The spatial variation of the intensity has a characteristic length, ξ_s , which is the speckle size and is simply related to the beam size d , the wavelength of the light λ , and the distance from sample to screen l in the same way as for interference from two slits separated by the distance corresponding to the beam size [11]

$$\xi_s \approx \frac{\lambda l}{d}. \quad (2.3)$$

If we plot the intensity as a function of vertical position (z_s) on the screen we would have something like the results in Fig. 2. The intensity fluctuations are correlated over ξ_s . In fact the intensity-intensity correlation function for two positions r_s and r'_s on the screen decays as [10]

$$\langle I(r_s)I(r'_s) \rangle = \langle I \rangle^2 \frac{\sin^2(2\pi|\mathbf{r}_s - \mathbf{r}'_s|/\xi_s)}{(2\pi|\mathbf{r}_s - \mathbf{r}'_s|/\xi_s)^2}. \quad (2.4)$$

We can also measure the intensity at a fixed point on the screen while displacing the sample in the beam. The result is schematically shown in Fig. 2, where z is the vertical coordinate of the sample. If both the sample and the beam were displaced together, with the same scatterers illuminated, the speckle pattern would not change at all. If the scatterers occupied a region smaller than the beam size and they were rigidly translated in the beam the speckle pattern would again remain unchanged. However, when a bulk sample is moved, some of the scatterers move out of the beam while the others move into it. The intensity remains correlated until most of the illuminated scatterers have been replaced. Thus the characteristic distance is the beam width, and the intensity-intensity correlation function is (see Appendix A)

$$\langle I(0)I(z) \rangle = \langle I(0) \rangle^2 [1 - n(z)/N]^2, \quad (2.5)$$

$$1 - n(z)/N \sim e^{-4z/\pi d}.$$

If the scatterers are randomly distributed, then the full Gaussian statistics are reflected in the correlation function in Eq. (2.4) and Eq. (2.5) and their relation to the average intensity, i.e., translating the detector or moving the sample result in the same average intensity and the rms fluctuations are equal to the average intensity $\langle \delta I^2 \rangle / \langle I \rangle^2 = 1$.

Now we want to see what happens when the scatterers can move. At one instant of time, if we take a snapshot of the screen, we would find something that looks like the static case. We follow the intensity at two different points on the screen, say z_{s1} and z_{s2} in Fig. 3. The variation of intensity with time for these points is shown schematically for an ergodic system. In such a system the time evolution of the particles leads the system through the configurations of the statistical ensemble, the fluctuations are just those of the random arrangement of positions. Each point on the screen undergoes a similar evolution of intensities with the same average and deviations. A time exposure photograph would show no spatial variation. The temporal fluctuations are correlated over the time it takes a scatterer to randomly displace a

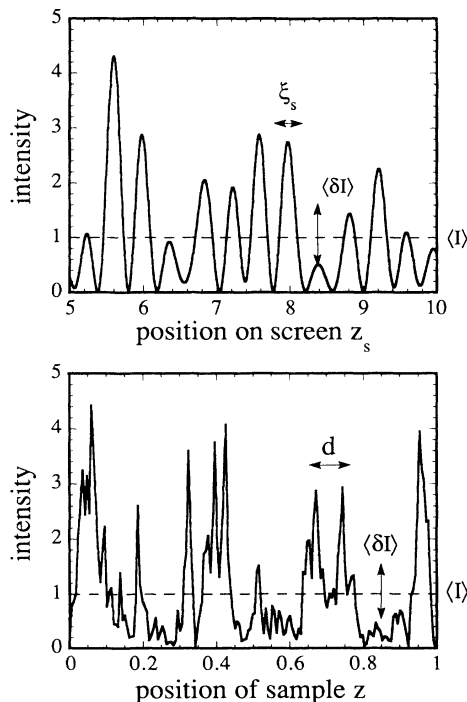


FIG. 2. (Top) For a static sample the intensity measured on the screen fluctuates (as the detector point is translated) about its mean value $\langle I \rangle$ with a variance $\langle \delta I \rangle$ which is equal to the mean, giving rise to the speckle pattern. The speckles are spatially correlated over a “speckle size.” (Bottom) The intensity of a fixed spot on the screen fluctuates with the full variance when the sample is translated. In this case the correlation length is \approx beam diameter divided by π .

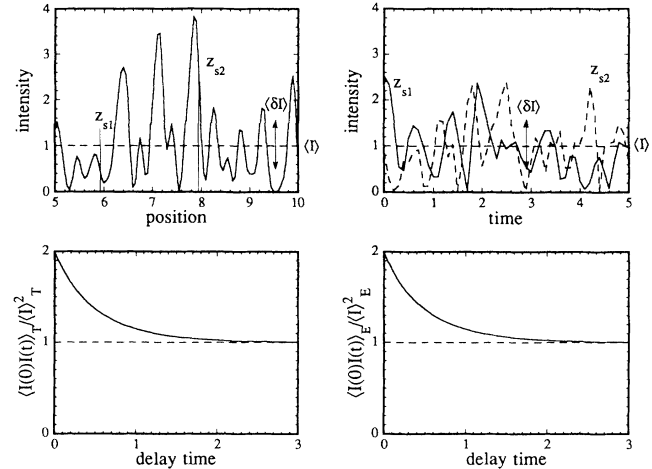


FIG. 3. Spatial and temporal behavior for an *ergodic* system. (Upper right) Snapshot of the intensity on the screen showing full variance with position. (Upper left) Time dependence of the intensity at two points on the screen (z_{s1} and z_{s2}) also shows full variance in the fluctuations. In both figures, $\langle I \rangle$ indicates the average scattering intensity and $\langle \delta I \rangle$ its variance. (Lower left) The ensemble-averaged correlation function shows the full variance at $t = 0$ and the decay of all correlations after several characteristic relaxation times. (Lower right) The time-averaged correlation function is the same as time-averaged correlation function in this case.

distance $2\pi/q$. At sufficiently long times the system has evolved to a configuration which is completely uncorrelated with its initial configuration so that

$$\langle I(0)I(\infty) \rangle = \langle I(0) \rangle \langle I(\infty) \rangle = \langle I(0) \rangle^2. \quad (2.6)$$

Time averages and ensemble averages are equivalent and the intensity correlation function with time is as illustrated schematically in Fig. 3.

If not all of the scatterers are free to explore the entire space of the sample then the time evolution of the system will not lead to all of the statistically possible configurations of the particles. The system is nonergodic [5] and there is no reason why the time and ensemble averages have to be the same. To illustrate how this affects the light scattering we again imagine taking a snapshot of a screen on which the scattered light falls and then watching its time development. The snapshot is illustrated in Fig. 4, and shows the position-dependent intensity with the full ensemble variance. We now look at the intensity vs time for two arbitrary points on the screen, z_{s1} and z_{s2} . If nothing in the sample is moving the intensity is independent of time. If every scatterer is moving randomly over distances larger than the wavelength of light λ , then the intensities will fluctuate with time much as for the ergodic system described above. However, if their motion is restricted to less than λ or if only some scatterers move, then the temporal averages and fluctuations will not be independent of the spot on the screen chosen for study. Similarly a time exposure of the intensity will not be uniform across the screen. (The schematic time

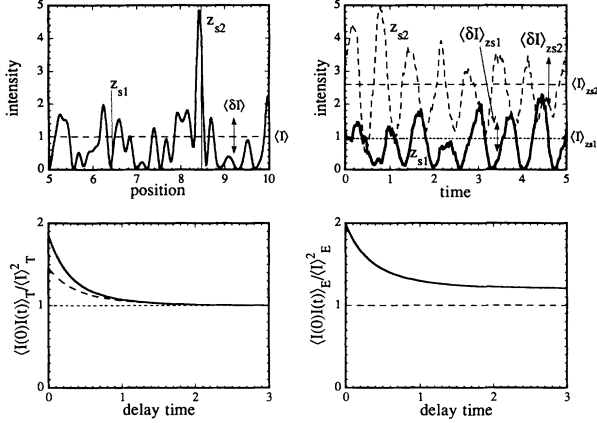


FIG. 4. Spatial and temporal behavior for a *nonergodic* system. (Upper right) Snapshot of the intensity on the screen showing full variance with position. (Upper left) Time dependence of the intensity at two points on the screen (z_{s1} and z_{s2}) also shows limited range in the fluctuations with a different average and variance at the two points. $\langle I \rangle$ and $\langle \delta I \rangle$ represent the average scattering intensity and its variance, respectively. (Lower right) The time-averaged correlation function depends on the position and is different for the two points illustrated. It is characterized by a reduction in the variance at short times. (Lower left) The ensemble-averaged correlation function is independent of position (it averages over position), is distinct from the time average, and shows the full variance at $t = 0$ and the persistence of some correlations for infinite time.

and position dependences shown in Figs. 3 and 4 were obtained by computing the intensity at different q 's for scattering from a set of 100 particles undergoing random or restricted walks, respectively.)

Most importantly, the time-averaged and ensemble-averaged correlation functions will be different. The range of the time-averaged correlation function is from unity at infinite time to one plus the fluctuations at $t = 0$:

$$\frac{\langle I(0)I(0) \rangle_T}{\langle I \rangle_T^2} = \frac{\langle I^2 \rangle_T}{\langle I \rangle_T^2} = \frac{\langle \delta I^2 \rangle + \langle I \rangle^2}{\langle I \rangle^2} \leq 2, \quad (2.7)$$

$$\frac{\langle I(0)I(\infty) \rangle_T}{\langle I \rangle_T^2} = \frac{\langle I(0) \rangle_T \langle I(\infty) \rangle_T}{\langle I \rangle_T^2} = \frac{\langle I \rangle_T^2}{\langle I \rangle_T^2} = 1. \quad (2.8)$$

For the ensemble average, the rms fluctuations are equal to the mean so that the ensemble-averaged correlation function goes to 2 at $t = 0$. For a nonergodic system, the time-averaged fluctuations at a fixed point on the screen are smaller than the ensemble average. Therefore, the time-averaged correlation function can be below 2 at zero delay time ($t = 0$) and will depend on the position of the detector and the particular orientation of the sample (see Fig. 4). A commercial correlator usually directly presents the time-averaged correlation function. In Fig. 5 we show the output of our correlator for the same sample in two orientations. It is clear that there is no way of gaining useful data directly from a correlation function which depends randomly on sample orientation.

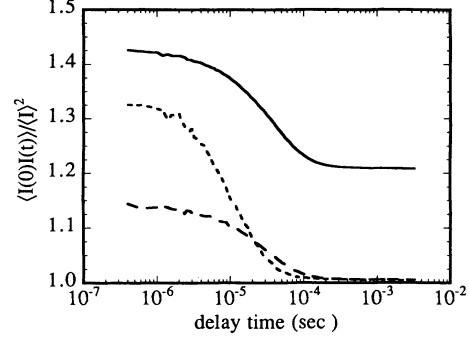


FIG. 5. Time-averaged correlation functions obtained for two different orientations of a nonergodic sample (dashed curves, obtained from one of our gel samples) compared with the ensemble-averaged correlation function (solid curve).

By contrast the correlation function that would naturally be calculated and that represents the global structure and dynamics of the system is the ensemble average. At $t = 0$ it contains the full fluctuations of the system and thus begins at 2. However, for the nonergodic system the fluctuations from $\langle I \rangle_E$ remain as $t \rightarrow \infty$ showing that the system does not lose its correlations. Thus the ensemble-averaged correlation function remains above unity:

$$\frac{\langle I(0)I(0) \rangle_E}{\langle I \rangle_E^2} = \frac{\langle I^2 \rangle_E}{\langle I \rangle_E^2} = \frac{\langle \delta I^2 \rangle + \langle I \rangle^2}{\langle I \rangle^2} = 2, \quad (2.9)$$

$$\frac{\langle I(0)I(\infty) \rangle_E}{\langle I \rangle_E^2} \geq 1.$$

In many cases, the long-time correlations are of interest. For example, in gelation, the glass transition, and solidification, the signature of the transition is the appearance of long-time correlations. Thus we would like to find a way to get the ensemble average.

The intensity-intensity correlation function can be written in terms of the electric-field correlation function as [5]

$$\begin{aligned} \langle I(0)I(T) \rangle &= \langle |E(0)E^*(t)|^2 \rangle + \langle I \rangle^2, \\ F(q, t) &= \langle E(0)E^*(t) \rangle = \sum_{j,k} \langle e^{i\mathbf{q} \cdot [\mathbf{r}_j(0) - \mathbf{r}_k(t)]} \rangle, \end{aligned} \quad (2.10)$$

$$\begin{aligned} f(q, t) &= F(q, t)/F(q, 0), \\ \frac{\langle I(0)I(t) \rangle}{\langle I \rangle^2} &= 1 + |f(q, t)|^2. \end{aligned}$$

In most cases the dynamical information about the system that is of most interest is directly contained in the function $f(q, t)$. We emphasize that in a nonergodic system $f(q, \infty)$ is not necessarily 0.

In previous papers on nonergodic systems, the authors [8, 9] came up with a clever way of obtaining the ensemble-averaged correlation function basically by evaluating the fluctuations with time as compared with the fluctuations with different configurations. We follow their presentation. Assume that each scatterer has in general

a static R_j and dynamic $\Delta_j(t)$ part to its position. The scattered field and intensity then also have static $E_C(q)$ and fluctuating $E_F(q, t)$ pieces:

$$E(q, t) = \sum_j e^{i\mathbf{q}\cdot\mathbf{R}_j + \Delta_j(t)} = E_F(q, t) + E_C(q). \quad (2.11)$$

The time-averaged intensity has a contribution from the static and fluctuating parts:

$$\langle I(q) \rangle_T = \langle |E(q, t)|^2 \rangle_T = \langle I_F(q, t) \rangle_T + I_C(q). \quad (2.12)$$

Now we look only at the fluctuating parts. The time-averaged correlation function, resulting from the fluctuating part of the electric field, is reduced from the ensemble average since $f(q, \infty)$ is not 0:

$$\langle E_F(q, 0)E_F^*(q, t) \rangle_T = \langle I(q) \rangle_E [f(q, t) - f(q, \infty)], \quad (2.13)$$

$$\langle I_F(q) \rangle_T = \langle I(q) \rangle_E [1 - f(q, \infty)]. \quad (2.14)$$

Likewise the time average of the fluctuating part of the intensity is less than the ensemble average. The fluctuating part of the intensity-intensity correlation function is obtained from that of the electric field by noting that the time-dependent part of the electric-field correlation beats against itself in a homodyne manner and beats against the static part of the intensity in a heterodyne manner [5, 11]:

$$\begin{aligned} \langle I(0)I(t) \rangle_T - \langle I \rangle_T^2 &= \langle I \rangle_E^2 [f(q, t) - f(q, \infty)]^2 \\ &\quad + 2I_C \langle I \rangle_E [f(q, t) - f(q, \infty)]. \end{aligned} \quad (2.15)$$

Thus the function $f(q, t)$ can be obtained if we know the time-averaged intensity relative to the ensemble averaged intensity:

$$Y \equiv \frac{\langle I \rangle_E}{\langle I \rangle_T}. \quad (2.16)$$

The parameter Y can be obtained by measuring the time-averaged intensity inside the speckle spot where the correlation function is taken, and then opening the aperture to the photodetector to collect light from many speckles. The relationship becomes

$$\begin{aligned} \frac{\langle I(0)I(t) \rangle_T}{\langle I \rangle_T^2} &= 1 + Y^2 [f^2(q, t) - f^2(q, \infty)] \\ &\quad + 2Y(1 - Y)[f(q, t) - f(q, \infty)]. \end{aligned} \quad (2.17)$$

Knowing the fluctuating part of the correlation function allows evaluation of $f(q, t) - f(q, \infty)$ and knowing that $f(q, 0) = 1$ allows evaluation of $f(q, \infty)$.

There is a less clever, more direct way of getting at the ensemble average which we have used in the present study. It consists of simply translating the sample to obtain data from a number of configurations. The characteristic decorrelation time is given in Eq. (2.5) and corresponds to a new ensemble for each τ . In order to make the demonstration simple we make the ensemble-averaging

time much longer than the longest decay time in the fluctuating part of the correlation function. A comparison of different ways of arriving at the desired ensemble-averaged time-dependent intensity-intensity correlation function is shown in Fig. 6.

In Fig. 6 (top) the direct signal from the correlator is presented. The sample is fixed in place and the correlator software interprets the time-averaged correlation

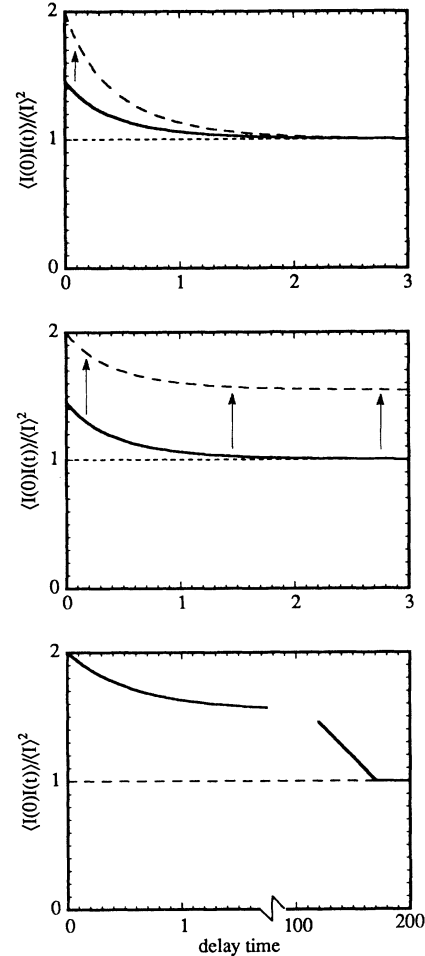


FIG. 6. Schematic of three possible ways of adjusting the time-averaged correlation function for data taken on a non-ergodic system. (Top) The incorrect way is to assume the baseline is correct and simply scale up the measured correlation function (solid curve) from the baseline so that the $t = 0$ value has the full variance of 2 (dashed curve). Although this is what correlator software and most experimentalists will do, it introduces uncontrolled factors in the analysis. (Middle) The method of Joosten *et al.* [9] is to find a speckle where the intensity is the ensemble-average intensity. In this case the fluctuating part of the measured correlation function (solid curve) is correct and the correct correlation function is obtained by shifting the curve up so the $t = 0$ value is 2 (dashed curve). (Bottom) The method we use here consists of moving the sample to ensemble average directly. The correlation function is ensemble averaged on a time scale corresponding to a sample translation by an illuminating beam diameter (d/v) and the ensemble-averaged correlation function is obtained from the data at shorter times.

function as being of the form

$$\frac{\langle I(0), I(t) \rangle}{\langle I(0) \rangle^2} = 1 + \beta^2 |f(q, t)|^2 \quad (2.18)$$

with $f(q, \infty) = 0$ (see Appendix B). It therefore takes the time correlation function and fixes the long-time part at unity and scales $\langle I^2(0) \rangle / \langle I(0) \rangle^2$ according to $1 + \beta^2$. Since the data depend on the orientation of the sample and changes when the sample is placed in a new position, this way of looking at the data is incorrect in a completely uncontrollable way.

In Fig. 6 (middle), we illustrate the clever technique for the particular case where the scattered light is detected at a spot where the time-averaged intensity and the ensemble-averaged intensity are equal. This situation can easily be obtained by measuring $\langle I \rangle_E$ first and then finding a spot where the scattering intensity (count rate), $\langle I \rangle_T$, is the same as $\langle I \rangle_E$. In this case the time average and the ensemble average of the time-dependent part of the correlation function are the same. In order to find the ensemble-averaged correlation function it is simply necessary to shift the *entire* curve up until the $t = 0$ point equals 2. This sets the entire correlation function, and in particular the shift is just $f(q, \infty)$.

In Fig. 6 (bottom), we illustrate our technique. The usual software of the correlator correctly sets the long-time behavior to unity and expands the $t = 0$ behavior to 2. The long plateau from the characteristic relaxation time of the dynamic part of the scatterers motion to the ensemble-averaging time correctly yields the value of $f(q, \infty)$. As shown in the Appendixes, this simple technique yields as good statistics as the clever scheme above while avoiding the constraints of that method. In particular it is not necessary to limit the detector aperture to a speckle size or less. The direct ensemble averaging is straightforwardly performed for any sample where conventional light scattering is done with no further adjustment than a slow translation (or rotation) of the sample. That the sample dynamics and ensemble-averaging times

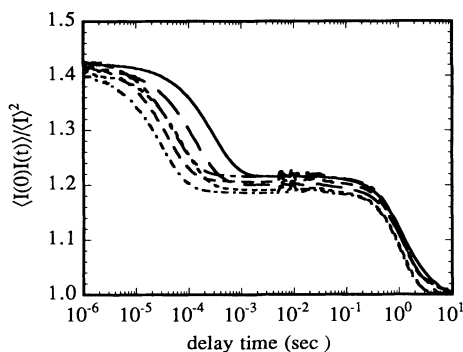


FIG. 7. Time-averaged intensity-intensity correlation function for several different q vs log times directly as taken by the correlator for a gel, ensemble averaged by translating the sample. From right to left, the scattering angles are 30° , 45° , 60° , 75° , 90° , and 105° . Note the well-separated time scales for the dynamics of the system ($\sim 10^{-4}$ sec) and the ensemble averaging (~ 1 sec).

can be readily separated is easily observed in the data of Fig. 7.

III. WHY GELS ARE DYNAMIC AND NONERGODIC

What makes gels interesting and distinct from other forms of matter is the property that they are sufficiently cross linked so that they do not flow (with sufficiently small applied stress). They are thermodynamically stable amorphous solids [12]. Equivalently they have a finite shear modulus or rigidity [3, 13]. We would therefore expect that the part of the network responsible for the rigidity must have some permanence and that each piece of it cannot translate infinitely far away from its initial position. The elastic part of the network can contribute to the light scattering in two ways. If the network is optically homogeneous then the only scattering is from thermal density fluctuations — thermal excitation of gel modes. A density fluctuation will scatter light and then decay into the uniform nonscattering background. There is no long-time correlation in the scattered intensity and the fluctuations form an ergodic subsystem.

On the other hand, neutron-scattering techniques have shown that polymer gels are inhomogeneous [14]. The inhomogeneities are frozen-in fluctuations from the uniform ensemble average, and may be sufficiently large to scatter light even in the absence of thermal fluctuations. The statistical ensemble consists of all possible preparations of the gel. Each will have its own particular inhomogeneities. Experimentally, the inhomogeneities may be regions of the network with a slightly different density of polymer vs solvent. They can move around with a Brownian-like motion, but since they are part of the rigid network they cannot move very far. If they do not move at all then their correlation function is time independent and finite. If they move somewhat then the scattered intensity is completely correlated instantaneously but decays to a nonzero value at long times.

There also may be scattering from material which is not part of the rigid network. If the pieces are small enough then they may undergo some simple or hindered diffusion. If they are large then they may be trapped in the network and resemble inhomogeneities of the network itself. In general there is no reason to expect that the scattered light does not consist of a mixture of all of these contributions. However, it is convenient to view the system in terms of two distinct paradigms to separate the dominant contributions and see whether light scattering can provide some quantitative information about particular gel systems. Since light scattering from most gels shows a speckle pattern which appears static to casual visual inspection, there are certainly both static and dynamic components. The two contrasting paradigms are then:

- gel modes plus a static background (dirt),
- harmonically bound Brownian particles.

A. Gel modes plus dirt

The gel modes and their contribution to light scattering have been extensively studied by many groups starting with Tanaka. Following his notation the equation for the displacement field, \mathbf{u} , is [1, 15]

$$\rho \frac{\partial^2 \mathbf{u}}{\partial t^2} = \mu \nabla^2 \mathbf{u} + (\kappa + \frac{1}{3}\mu) \nabla(\nabla \cdot \mathbf{u}) - f \frac{\partial \mathbf{u}}{\partial t}. \quad (3.1)$$

The inertial term on the left is driven by stresses from the shear and bulk elasticity and Stokes-like viscous friction. The elastic stress is from the rigid network while the friction is from the relative motion of the solvent and the network. There are several solutions to these equations corresponding to “fast” modes ($-i\omega = f/\rho$ from $\rho \ddot{\mathbf{u}} = -f\dot{\mathbf{u}}$) or inertial relaxation to the viscous fluid, and “slow” modes [$-i\omega = (\kappa + 4/3\mu)q^2/f$, from $f\dot{\mathbf{u}} = (\kappa + 4/3\mu)(\partial^2 \mathbf{u}/\partial z^2)$] or elastic relaxation in the viscous fluid. The fast modes, with a damping time of 10^{-7} sec [1], are outside the time range accessible to even present day correlators, so we concentrate on the slow modes. To calculate the light scattering from these modes we note that the uniform displacements do not produce changes in density, rather their gradients do. Therefore the electric-field correlation function is proportional to the correlation function of the gradient of the displacement:

$$\langle E_q(0)E_q^*(t) \rangle \propto \langle \nabla U_q(0) \nabla U_q(t) \rangle \sim q^2 \langle U_q(0)U_q(t) \rangle, \quad (3.2)$$

$$\langle U_q(0)U_q(t) \rangle = \langle U_q^2(0) \rangle e^{-Gq^2 t/f}, \quad (3.3)$$

where $G = \kappa + 4/3\mu$, and $U_q(0)$ is the amplitude of the gel modes. The result is a simple exponential decay with a single time constant proportional to $1/q^2$ as for a diffusive process. We appeal to equipartition to find the amplitude of the modes:

$$\rho \frac{\omega_q^2 \langle U_q^2 \rangle}{2} = \frac{Gq^2 \langle U_q^2 \rangle}{2} \propto \frac{k_B T}{2}, \quad \langle U_q^2 \rangle \sim \frac{k_B T}{Gq^2}, \quad (3.4)$$

$$\langle E_q(0)E_q^*(t) \rangle \propto \frac{k_B T}{G} e^{-Gq^2 t/f}. \quad (3.5)$$

The electric-field correlation function looks like that of a diffusive mode whose amplitude is independent of q . If we do not look especially at depolarized light scattering then the scattered light we observe is from the longitudinal modes which give density fluctuations rather than the shear modes which do not affect the density.

The gel modes by themselves give a correlation function which decays to zero at long times. This correlation function is the correct ensemble average for a system which has as its equilibrium configuration no static inhomogeneities which scatter. However, the typical gels studied have frozen in structures. It may be that the system of interest is the ensemble with these structures removed, or it may be that these inhomogeneities are of interest in the study and should therefore be considered as part of the statistical ensemble since they are different

allowable manifestations of the gel. In either case the effect of the frozen structures is to provide a static electric field which interferes directly with the electric field from the gel modes. The effect is the same as for a heterodyne experiment with a static reference:

$$\langle E_q(0)E_q^*(t) \rangle \propto \frac{A + Be^{-Gq^2 t/f}}{A + B}, \quad (3.6)$$

where A is due to scattering from the illuminated inhomogeneities, and B is due to scattering from the gel modes [1]:

$$B \propto \phi^2 \frac{kT}{G} \propto \phi^{-1/4}. \quad (3.7)$$

The last proportionality in Eq. (3.7) holds for polymer gels in a good solvent [16]. Whether the static part is considered interesting or not it must be taken into account in analyzing the dynamic part especially because A is different for every position or orientation of the sample.

B. Harmonically bound Brownian particles

If the dynamic part of the light scattering comes from the motion of uncorrelated scatterers (as distinct from the gel modes problem where there is no scattering until a thermal fluctuation creates a density gradient), then the calculation of the electric-field correlation function is direct:

$$\begin{aligned} \langle E_q(0)E_q^*(t) \rangle &= \left\langle \sum_{i,j} e^{i\mathbf{q} \cdot [\mathbf{r}_i(0) - \mathbf{r}_j(t)]} \right\rangle \\ &= \sum_i e^{-q^2 \langle \delta r_i^2(t) \rangle / 6}, \end{aligned} \quad (3.8)$$

where we have assumed that $\mathbf{q} \cdot \delta \mathbf{r}$ is a Gaussian random variable. For a freely diffusing particle as a scatterer we would have

$$\langle \delta r^2(t) \rangle = 6Dt, \quad (3.9)$$

where $D = k_B T / 6\pi\eta a$ is the diffusion constant, η is the solvent viscosity, and a is the particle radius. The correlation function is a simple exponential with a time constant varying inversely with q^2 and an amplitude which is independent of q . In form it is indistinguishable from that of the gel modes. If the scatterers are bound or trapped in the gel network then they cannot diffuse infinitely far. If we imagine starting from the equilibrium position then there is no restoring force from the network and the scatterer diffuses as a free particle. However, on leaving its equilibrium position it encounters the network restoring force. The maximum displacement from equilibrium is when the elastic energy is equal to the thermal energy or $K \langle \delta r^2(\infty) \rangle / 2 = K \langle \delta^2 \rangle / 2 = k_B T / 2$, where K is the effective spring constant of the gel network on the scatterer. The problem of the “harmonically bound Brownian particle” (HBBP) has been solved several times in the literature and the time dependence of the displacement is [7]

$$\langle \delta r^2(t) \rangle = \langle \delta^2 \rangle (1 - e^{-t/\tau_B}), \quad \tau_B = \frac{6\pi\eta a}{K}, \quad (3.10)$$

where η is the viscosity, K the spring constant, and a the particle radius. This gives an electric-field correlation function as

$$\langle E_q(0)E_q^*(t) \rangle \propto e^{-q^2 \langle \delta^2 \rangle (1 - e^{-t/\tau_B})}. \quad (3.11)$$

The correct ensemble-averaged correlation functions for the two cases we consider are shown schematically in Fig. 8. The time dependence of $f(q, t)$ is very similar for the gel modes plus dirt or for the harmonically bound particle. For the gel modes plus dirt model the initial decay of the correlation function is linear with time and depends not only on the elasticity and viscosity but also on the relative amount of static and dynamic scattering. For the HBBP model the initial linear decay is directly the diffusion constant. The saturated value $f(q, \infty)$ is determined by the ratio of static to total scattering for the gel modes case and the limited motion of the particle for the HBBP case. A single ensemble-averaged experiment cannot distinguish the two with any reasonable accuracy. The real test is in the scattering wave-vector dependence. In Fig. 8 we also show how the two cases separate when q is varied.

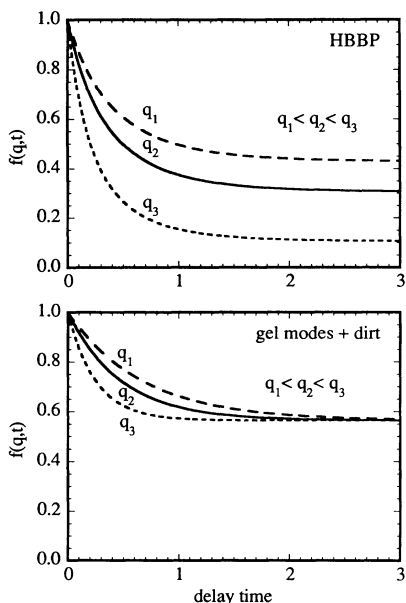


FIG. 8. The scattering function vs time for a typical nonergodic system can be interpreted in terms of diffusing particles or damped modes plus dirt or by the motion of a bound Brownian particle. The signature of the two different behaviors is found in the q dependence. (Top) For the harmonically bound Brownian particle the entire deviation from unity scales exponentially with q^2 while the characteristic time is independent of q . (Bottom) For the dynamics plus dirt model the baseline is independent of q (if the static scatterers are much smaller than q^{-1}) while the characteristic time scales inversely with q^2 .

IV. EXPERIMENTS ON POLYACRYLAMIDE GELS

We have studied polyacrylamide gels prepared as in the published literature [1, 17]. We prepared solutions of each component by dissolving 4.37-g acrylamide (M), 0.135-g bisacrylamide (C), 36-mg ammonium persulfate, and 154- μ l tetramethyl-ethylene-diamine (TEMED) in 20 ml of water, respectively. The solutions are then filtered using a 0.22- μ m filter, and mixed in glass tubes. By fixing the relative proportions of each component and by adding distilled and deionized water, gels with different total monomer concentrations are prepared. The crosslink concentration $[C/(M + C)]$ for all gels is 3% by weight, and the total monomer concentration ($M + C$) varies from 4.3% to 2.45% by weight. Although the gelation process takes about 1 h to complete at room temperature, our gels were sealed in light-scattering glass tubes about 1 cm in diameter and studied 30 days after preparation. All gels were clear and homogeneous by visual inspection.

Other than the important modification of mounting the sample on a rotation and translation stage via a rubber necking, the experimental setup for our experiments was the same as for a conventional dynamic-light-scattering experiment. A He-Ne laser with wavelength $\lambda = 6328 \text{ \AA}$ in *vacuo* is used as the light source. The detector, goniometer, and oven system we used was a Brookhaven Instrument light-scattering apparatus (Model BI 200 SM). We used an ALV5000 correlator to measure the correlation functions. The temperature of the samples was set to be 25 $^{\circ}\text{C}$.

The ensemble-averaged intensity-intensity correlation function for several values of the scattering wave vector q as directly output from our correlator is shown in Fig. 7 for one of the gels we studied. Our correlator normalizes the correlation function by the ensemble-averaged intensity squared rather than by the delayed correlation function at long times. Note that the abscissa is log time and that the two characteristic time scales are separated by more than three orders of magnitude. The long-time scale ~ 1 sec is determined by the ensemble-averaging procedure where the beam size is ~ 0.2 mm and the sample is translated at a velocity of ~ 1 cm/min and rotated at less than one revolution per hour. The short-time scale is determined by the dynamics of the system. The fact that the correlation function saturates to ~ 1.4 rather than 2 as $t \rightarrow 0$ results from the finite size of the aperture on our phototube. The aperture averages over several speckles and therefore reduces the fluctuations. In order to obtain the scattering function $f(q, t)$ from the data in Fig. 7 it is merely necessary to set the aperture function β^2 equal to the difference between $\langle I^2 \rangle$ and unity (i.e., in this case $\beta^2 = 0.4$ — β^2 was also measured to be 0.4 in other experiments with this particular geometry).

The scattering function obtained in this way for the gel is shown in Fig. 9. Comparison with Fig. 8 shows that the correct model for the gel scattering is gel modes plus dirt. The characteristic decay time is very q dependent while the static part of the scattering $f(q, \infty)$ is q

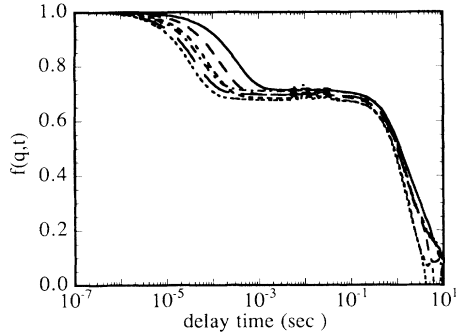


FIG. 9. Scattering function for several values of q obtained from the data of Fig. 7. The scattering angles are in the same order as in Fig. 7.

independent. To make this statement more quantitative we plot the q dependence of $f(q, \infty)$ in Fig. 10 (top left) for five different gels. We see that there is less than 5% variation instead of the strong exponential dependence expected for the HBBP model.

The q dependence of the initial slope of $f(q, t)$ is shown in Fig. 11. The q^2 dependence from either model is clearly demonstrated. The slopes of the curves give the

ratios of the elastic constant to the viscosity for the different gels. To further elucidate the difference between the two models, we show the full scattering function $f(q, q^2 t)$ vs $\log(q^2 t)$ in Fig. 12. Scaling the time with q^2 we see that the data collapse, so that the characteristic time varies as q^2 . Moreover, the measured $f(q, t)$ are very well represented by the form $\exp[(-t/\tau)^\beta]$ with $\beta = 1.00 \pm 0.05$, i.e., a single exponential.

We also measured the static scattering intensity $I(q)$ for all gels as a function of q . From our measurements of $f(q, \infty)$, we extract the contributions to $\langle E_q(0)E_q^*(t) \rangle$ from the static inhomogeneities and the gel modes; these are given by $A(q) \equiv I(q)f(q, \infty)$ and $B(q) \equiv I(q)[1 - f(q, \infty)]$, respectively [see Eq. (3.6)]. In Fig. 10 (top right) we plot $B(q)$ for all five gels we studied. Notice that $B(q)$ is essentially independent of q and the total monomer concentration ϕ , in agreement with Eq. (3.7). However, we find that $A(q)$, the scattering from the inhomogeneities, is strongly concentration dependent, but weakly q dependent, as shown in Fig. 10 (bottom right and bottom left). The weak q dependence suggests that the inhomogeneities are smaller than the wavelength of light. Using the Born approximation and modeling the inhomogeneities as independent spheres, we estimate the characteristic size ξ of the inhomogeneities from $A(q)$ and find that ξ ranges from 500 Å to 820 Å for the lowest and

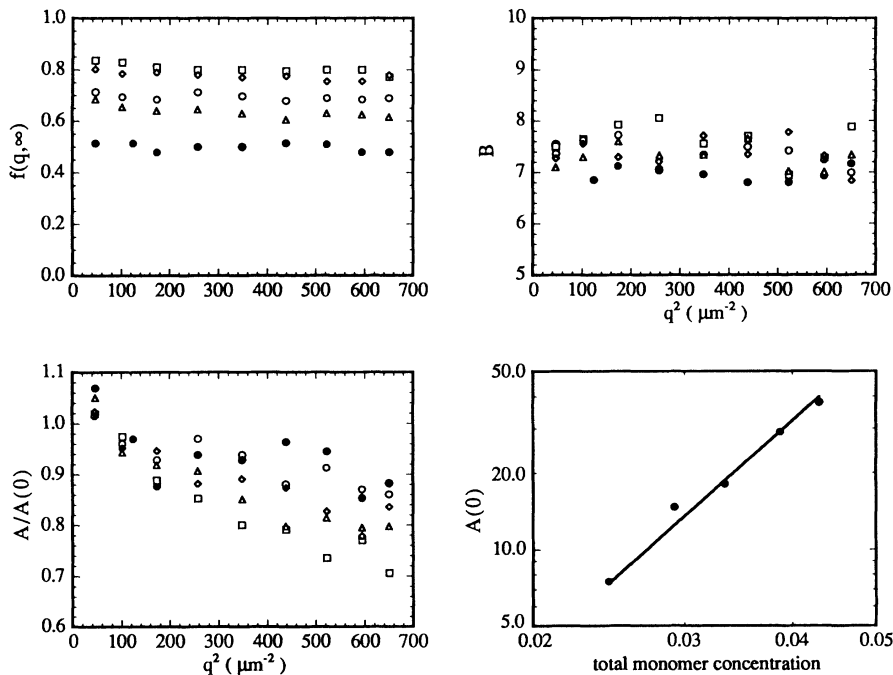


FIG. 10. (Top left) q dependence of the saturated long-time part of the scattering function $f(q, t)$ for five different polyacrylamide samples with different total monomer concentrations. (Top right) Static scattering intensity due to the gel modes as a function of q for the five gels. (Bottom left) The q dependence of the static scattering intensity due to inhomogeneities for the five gels. The scattering intensities are normalized by the extrapolated $q = 0$ value. In these three figures, the symbols represent total monomer concentrations at 4.3% (\square); 3.87% (\diamond); 3.34% (\circ); 2.92% (\triangle); and 2.45% (\bullet). (Bottom right) The extrapolated static scattering intensity $A(q = 0)$ due to the inhomogeneities as a function of concentration. The symbols are for experimental data, and the solid line is a guideline with $A(0) \sim \phi^3$, where ϕ is the total monomer concentration. The unit of the vertical axes for the top right and bottom right is the same, although they are arbitrary.

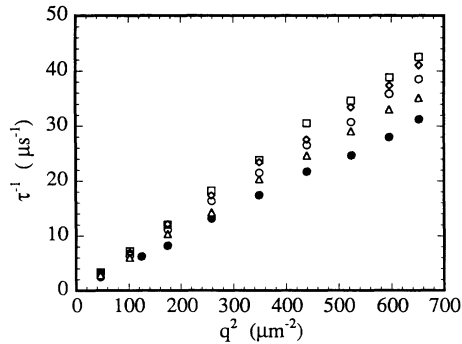


FIG. 11. q dependence of the initial slope of the scattering function showing the linearity with q^2 expected from either diffusion or damped modes. The symbols are the same as for Fig. 10.

the highest concentration gels. This increase in ξ should also lead to an increase in the static scattering from the inhomogeneities; in the Born approximation, the scattering power is proportional to ξ^6 . Since the scattering is proportional to the number of scatterers, we expect that $A(q=0) \sim \phi \xi^3$. Our measurements suggest that $\xi \sim \phi^{0.8 \pm 0.2}$ and that $A(q=0) \sim \phi^3$ (Fig. 10); this is consistent (to within significant uncertainty) with the crude model suggested above.

On the other hand, if the inhomogeneities are too small then they should move in the gel matrix as harmonically bound Brownian particles and we should again see a q dependence of $f(q, \infty)$. From our measurements, we observe about a 5% change in $f(q, \infty)$. Using Eq. (3.11), we estimated that the inhomogeneities move less than 100 Å. We should note that if the scattering is completely from harmonically bound Brownian particles, then A and B should have the same concentration dependence.

The results of this study are thus conclusive: the gels we have made are fairly strong gels with frozen in inhomogeneities whose dynamics is dominated by the gel modes. The scattering function is very well represented by Eq. (3.6).

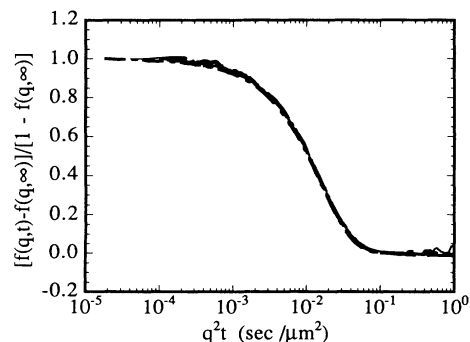


FIG. 12. The data in Fig. 9 have been replotted as a function of $q^2 t$ to show that this makes the curves for different q collapse.

V. HOW COULD ANYONE GET THE RIGHT ANSWER WITHOUT ENSEMBLE AVERAGING?

There have been extensive studies of light scattering from polymer gels and other gel systems [1, 2, 17–20]. With the exception of Joosten *et al.*'s work none of them addressed the problem of ensemble averaging [9]. Now that we know the origin of the scattering in the gel, we can see what the result of time averaging without sample translation would be. A correlator assumes that it is seeing a signal of the form

$$\frac{\langle I(0)I(t) \rangle_T}{\langle I \rangle_T^2} = 1 + \beta_{\text{eff}}^2 G_{2\text{eff}}. \quad (5.1)$$

The ensemble average G_2 from our measurements is

$$G_{2\text{ens}} = (A + B e^{-t/\tau})^2 / (A + B)^2. \quad (5.2)$$

If instead of ensemble averaging we were to look at scattering from a single realization of the ensemble (i.e., the detector sits at a particular position z_s on the screen), we would have

$$G_{2z_s} = (A_{z_s} + B e^{-t/\tau})^2 / (A_{z_s} + B)^2, \quad (5.3)$$

where the squared scattering function G_2 depends on sample position because the static part of scattering, A_{z_s} , depends on which static speckle is illuminating the detector. In this case, A_{z_s} fluctuates from zero to some unlimited value with an average that is $A = A_{\text{ens}}$. The correlator interprets the data as in Eq. (5.1), setting $\beta_{\text{eff}}^2 = \beta^2 B (2A_{z_s} + B) / [\beta^2 A_{z_s}^2 + (A_{z_s} + B)^2]$ and the correlation function as

$$G_{2\text{eff}} = \frac{2A_{z_s} e^{-t/\tau} + B e^{-2t/\tau}}{2A_{z_s} + B}. \quad (5.4)$$

Now the answer can be whatever the experimentalist wants since the sample can be oriented to get virtually any value for A_{z_s} . However, this will lead to quite irreproducible results. There are several choices. One way to obtain consistent results is to orient the sample to make A_{z_s} large and assume a heterodyne signal. Another way is to make A_{z_s} as small as possible and assume a homodyne signal. Once it is realized that the usual signal is a combination of homodyne and heterodyne, one can choose a subtraction for each sample that makes data taken from different measurements consistent [6]. Note that the possibility of obtaining the correct results for the dynamics of the system by any of these procedures only works in the case when the scattering involves dynamic plus static scattering. If the system were actually the harmonically bound Brownian particle there would be no correct way to interpret the data without doing the correct ensemble averaging.

There are other ways that experimentalists may have chosen to collect the light-scattering data. When one realizes that the scattering intensity changes for different placements of the sample, one might rotate the sample so that the count rate from the photon detector is roughly the same before every measurement. Although the data collected in this way are consistent (i.e., different measurements yield the same results), the analysis is incor-

rect unless the scheme suggested in Refs. [8, 9] is used to account for the nonergodicity of the system.

VI. CONCLUSIONS

There are two main points we wish to emphasize from this study. The first concerns the general problem of dynamic light scattering from nonergodic systems, the second concerns our particular findings for the polymer gels we have studied.

If you want to do light scattering from a system which may be nonergodic, the correct scattering or correlation function can be most directly and efficiently obtained by translating the sample in the incident laser beam so that different regions are illuminated while collecting data with a correlator in the usual way. The effect of the translation may be factored from the data using Eq. (B2).

Simply put, the best way to get the ensemble average is to directly ensemble average by averaging over different representations of the sample. In the body and appendices of this paper we have shown that the averaging time and signal-to-noise ratio are at least as advantageously obtained with this technique as others previously prescribed. Moreover, the present technique has the additional advantage that it can be used with arbitrary aperture size with no assumption about the dynamics (or lack of dynamics) at any time scale and for multiple-scattering experiments. If it is inconvenient to move the sample, then moving the detector over many speckles will have the same consequences but will necessitate a less well-defined scattering vector, q . [In this case the translation function Eq. (A7) has the argument vt/ξ_s rather than vt/d .]

For the particular gels we have studied we conclude that the scattering function is the result of a dynamic part due to thermal excitation of gel modes heterodyned with an essentially static part due to inhomogeneities in the network. An interpretation in terms of the other proposed mechanism, restricted motion of bound particles or inhomogeneities, is inconsistent with our results, especially the q dependence of the scattering function at long times.

ACKNOWLEDGMENTS

We would like to thank John Huang and James Sung for their generosity in letting us use their equipment. We would also like to thank David Weitz, Ping Sheng, and Gary Grest for many helpful discussions.

APPENDIX A: SAMPLE TRANSLATION FUNCTION

We now address the calculation of the time-averaged correlation function that we obtain by moving the sample while taking data with the correlator. We again want the electric-field correlation function. The basic idea is that when the sample is translated there are scatterers which leave the illuminated area (on the trailing edge of the beam area) and new scatterers which enter (on the leading edge). Since the beam width is macroscopic, we expect that there is no correlation between the new and old scatterers, and the scattered electric fields are correlated only from the scatterers which remain illuminated. It is clear that there should be no correlation remaining when the sample has been translated a beam diameter. The completely new set of scatterers represents a new manifestation of the ensemble and the time average therefore ensemble averages as well. However, there is a new decay time in the correlation function related to the time to traverse the beam.

At time t we imagine that N scatterers are in the beam and the electric field is given by

$$E(t) = \sum_i^N e^{i\mathbf{q}\cdot\mathbf{r}_i(t)}. \quad (\text{A1})$$

At a time τ later the positions of the scatterers may have changed, but the motion of the sample has left n of them out of the beam and replaced them with n' new ones. The scattered field is now

$$E(t+\tau) = \sum_i^N e^{i\mathbf{q}\cdot\mathbf{r}_i(t+\tau)} - \sum_k^n e^{i\mathbf{q}\cdot\mathbf{r}_k(t+\tau)} + \sum_l^{n'} e^{i\mathbf{q}\cdot\mathbf{r}'_l(t+\tau)}. \quad (\text{A2})$$

The electric-field correlation function is then directly

$$\langle E(t)E^*(t+\tau) \rangle = \left\langle \sum_{i,j}^{N,N} e^{i\mathbf{q}\cdot[\mathbf{r}_i(t)-\mathbf{r}_j(t+\tau)]} \right\rangle - \left\langle \sum_{i,k}^{N,n} e^{i\mathbf{q}\cdot[\mathbf{r}_i(t)-\mathbf{r}_k(t+\tau)]} \right\rangle + \left\langle \sum_{i,l}^{N,n'} e^{i\mathbf{q}\cdot[\mathbf{r}_i(t)-\mathbf{r}'_l(t+\tau)]} \right\rangle \quad (\text{A3})$$

The time averaging also directly averages over different ensembles. The last term in this equation is zero since the interfering scatterers are the new and old ones which are uncorrelated. If we further imagine that there are no correlations between different scatterers then the only terms which survive the ensemble averaging are the interferences of a particle with itself at a later time:

$$\begin{aligned} \langle E(0)E^*(t) \rangle &= \left\langle \sum_i^N e^{i\mathbf{q}\cdot[\delta\mathbf{r}_i(t)]} \right\rangle - \left\langle \sum_i^n e^{i\mathbf{q}\cdot[\delta\mathbf{r}_i(t)]} \right\rangle \\ &= [N - n(t)]e^{-q^2\langle\delta r^2(t)\rangle}. \end{aligned} \quad (\text{A4})$$

Here it is clear that we have assumed an *average* number of scatterers N and have explicitly written that the

average number of scatterers translated out of the beam increases with time. More generally if there are nontrivial correlations between dissimilar particles (on length scales smaller than the beam width) of the form

$$\left\langle \sum_{i,k}^{N,n} e^{i\mathbf{q}\cdot[\mathbf{r}_i(0)-\mathbf{r}_k(t)]} \right\rangle = n f(q, t), \quad (\text{A5})$$

then the normalized electric-field correlation function is [10]

$$\begin{aligned} \frac{\langle E(0)E^*(t) \rangle_{\text{time}}}{\langle I \rangle_{\text{time}}} &= (1 - n(t)/N) \frac{\langle E(0)E^*(t) \rangle_{\text{ens}}}{\langle I \rangle_{\text{ens}}} \\ &= (1 - n(t)/N) f(q, t). \end{aligned} \quad (\text{A6})$$

To complete this part we need an expression for $n(t)$. If we assume a circular beam of diameter d then

$$n(t)/N = \pi - 2 \arccos(vt/d) + \sin[2 \arccos(vt/d)]. \quad (\text{A7})$$

The function $1 - n(t)/N$ is plotted in Fig. 13. It has an initial linear decay. Also in this figure is the convolution of this function with a scattering function for exponential decay plus constant, $f(q, t) = (A + Be^{-t/\tau_0})/(A + B)$ (where we have arbitrarily chosen $B = 1 - A = 0.57$, $\tau_0 = 50 \mu\text{sec}$, and $d/v = 1 \text{ sec}$). This figure should be compared with the data shown in Fig. 9.

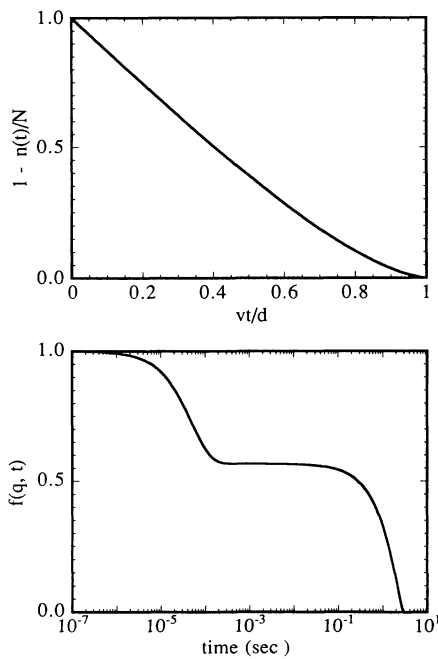


FIG. 13. (Top) The calculated intensity-intensity correlation function as a static sample is translated in the beam, using Eq. (A7). (Bottom) the calculated time-average correlation function for a nonergodic sample ensemble averaged by translation. Compare with the experiment plotted in Fig. 9.

APPENDIX B: FINITE APERTURE EFFECTS

Up to now we have assumed a point detector which would sample the light scattered at a particular q . Now we consider the role of a finite aperture on the photodetector. If we accept photons through a finite aperture then we are averaging over (or integrating over) a region of q space. The averaging will naturally reduce the fluctuations. Spatial correlations of the scattered intensity are characterized by the speckle size ξ_s at the detector. If the aperture is small compared to ξ_s we see the full variance. If the aperture is much larger than ξ_s then we accept many [$\approx (r/\xi_s)^2$ with r being the radius of the aperture] speckles. The magnitude of the fluctuations relative to the intensity decays as the square root of the number of speckles. More precisely the correct reduction in the magnitude of the fluctuations is given by integrating over q to obtain the aperture function β [21] where the conventional result for an ergodic system is written:

$$\frac{\langle I(0)I(t) \rangle_{\text{time}}}{\langle I \rangle_{\text{time}}^2} = 1 + \beta^2 | f(q, t) |^2, \quad (\text{B1})$$

and $\beta^2 \approx (r/\xi_s)^{-2}$ for $r \gg \xi_s$ and $\beta^2 \rightarrow 1$ for $(r\xi_s) \ll 1$. Since the effect of the finite aperture is taken into account by an integral over q , we see from Eqs. (A5) and (A7) that it is independent of the translation function $n(\tau)$, and therefore reduces $f(q, t)$ the same way as for an ergodic system.

Finally the relationship between the time-averaged intensity correlation function of the translated sample and the ensemble average of the static sample is

$$\frac{\langle I(0)I(t) \rangle_{\text{time}}}{\langle I \rangle_{\text{time}}^2} = 1 + [1 - n(t)/N]^2 \beta^2 | f(q, t) |^2. \quad (\text{B2})$$

It should be noted that the method of Refs. [8] and [9] cannot be used with a finite aperture in a simple manner. Although we have not explicitly demonstrated it here, Eq. (B2) is equally appropriate for the case of multiple scattering or DWS [22], where the method of [8] and [9] breaks down.

APPENDIX C: HOW LONG TO AVERAGE?

In principle, there are two factors that determine the error of the measured intensity-intensity correlation function. One factor is the signal-to-noise ratio related to the photon-counting statistics and dependent on the scattering intensity (see, for example, Ref. [23]). The other factor is the accuracy of the average correlation function which is related to the number of different system configurations (ensembles) included in the average. For a light-scattering experiment for an ergodic system, while collecting photons for a better signal-to-noise ratio, the system goes through many possible configurations resulting in different speckles, and the duration of measurements has to be long enough to give good statistics in both categories. For a nonergodic system, ensemble averaged by sample translation, the accuracy is determined directly by the number of independent systems

probed, which depends on the total length traversed by the beam. [Since by Gaussian statistics of the scattered light $\langle I(0)I(0) \rangle = 2\langle I(0)^2 \rangle$ or $f(q, 0) = 1$, the accuracy is primarily useful for determining $f(q, \infty)$ and thus is an interesting quantity only for nonergodic systems.]

The signal-to-noise ratio of the time-averaged intensity-intensity correlation function computed by a commercial correlator is simply the square root of the total number of counts in the channel. If the count rate (intensity) at the photodetector is n photons/sec and the channel width is τ sec, then the correlator computing $\langle I(0)I(t) \rangle$ increases the counts in the channel at a rate of $[(n\tau)^2/\tau][\langle I(0)I(t) \rangle / \langle I(0)^2 \rangle]$ counts/sec. The signal-to-noise ratio of the correlation function is just the reciprocal square root of the total number of counts after time T in the particular channel. Usually we are interested in the signal-to-noise ratio of $f(q, t)$ which we call σ^{-1} . We then have

$$\sigma^2 = \frac{1}{n^2\tau T} \frac{1 + \beta^2 f^2(q, t)}{4\beta^4 f^4(q, t)}, \quad (\text{C1})$$

where T is the measurement time.

For sample translation the accuracy with which we know $f(q, \infty)$, assuming that the noise due to photon statistics is sufficiently low, is the square root of the number of ensembles averaged. Since the scattered light is completely decorrelated when the sample is translated to a beam diameter, this number is just the path length divided by the beam diameter, or

$$N_{\text{ens}} = vT/d. \quad (\text{C2})$$

The additional constraint is that the characteristic time τ_c of the dynamics of the system should be long compared to the channel width. In most cases we also want τ_c short compared to the ensemble-averaging time d/v so that the "interesting" dynamics of the system are explored. (It is interesting to note however, that with ensemble averaging by translation the correct correlation function is obtained from Eq. (B2) even if the total sampling time or the longest delay time of the correlation function is shorter than τ_c . The result will simply be a correlation function which has not yet saturated as a function of delay time t , i.e., $f(q, t)$ will be correctly measured for $t < d/v$ but will be truncated after d/v). With τ_c at 10^{-5} sec, τ at 10^{-6} sec, $d = 0.1$ cm, $v = 0.01$ cm/sec, and $T = 10^3$ sec, all of the conditions are met with an accuracy and signal-to-noise ratio of better than 1%.

For completeness and for comparison, we also estimate the error in measured correlation functions using

the technique of Refs. [8] and [9]. The signal-to-noise ratio is determined again from photon-counting statistics. However, the information obtained about the long-time correlation $f(q, \infty)$ comes from the evaluation of the ratio $\langle I \rangle_{\text{ens}} / \langle I \rangle_{\text{time}} \equiv Y$. The accuracy of Y is the determining factor. The ensemble-averaged intensity is readily available by opening the aperture to the photon counter so that many speckles are sampled. The time-consuming part is evaluating the time average. If there is a characteristic time for the dynamics of the system, τ_c (and the a quasi-infinite time scale associated with the non-ergodicity), then to get $\langle I \rangle_{\text{time}}$ one must collect data for many τ_c . The accuracy is simply the inverse square root of T/τ_c :

$$\sqrt{N_{\text{time}}} = \sqrt{T/\tau_c}. \quad (\text{C3})$$

However, there is a fundamental problem which arises if the correlation function of the system and its dynamics are not known *a priori*. Suppose that the system is changing on a time scale comparable to or slightly longer than the measurement time, then the accuracy of the measurement is shot; that is, the uncertainty of $\langle I \rangle_{\text{time}}$ is 100%. Unless the dynamics and the characteristic times are known and expected there is an uncontrolled approximation in evaluating the correlation function. Note that the translational ensemble average does not have this problem. In fact the sample translation technique accurately gives the correlation function for time less than the cutoff time d/v even if the system is changing on any longer time scale.

To compare the time for data acquisition for the two techniques, we first note that, for Refs. [8] and [9], one has to use a small aperture to make sure β is larger. Cutting down the aperture reduces the count rate and, for the same signal-to-noise ratio, the time required for data collection when $\beta^2 = 0.95$ is about 10 times longer than when $\beta^2 = 0.4$. We also must use the assumption that we know *a priori* that there is a characteristic time τ_c and then saturation. In this case the Joosten *et al.*'s technique has an accuracy given by Eq. (C3). For the sample translation technique, knowing that there is a characteristic time scale after which there is nothing happening, it is most efficient to set the ensemble-averaging time to this time, i.e., $d/v = \tau_c$ in Eq. (C2). This makes the accuracy the same for the two measurements, but only under the assumption that we have *a priori* knowledge of the system dynamics. Otherwise the sample translation technique always wins.

[1] T. Tanaka, L.O. Hocker, and G.B. Benedek, *J. Chem. Phys.* **59**, 5151 (1973); T. Tanaka, *Phys. Rev. A* **17**, 763 (1978).
 [2] J.P. Munch, S. Candau, and G.J. Hild, *Polym. Sci. Polym. Phys. Ed.* **15**, 11 (1977).
 [3] R. Nossal, *Macromolecules* **18**, 54 (1985); R. Nossal and M. Jolly, *J. Appl. Phys.* **53**, 5518 (1982); R.A. Gelman and R. Nossal, *Macromolecules* **12**, 311 (1979).

[4] E.R. Duering, K. Kremer, and G.S. Grest, *Phys. Rev. Lett.* **67**, 3531 (1991).
 [5] B.J. Berne and R. Pecora, *Dynamic Light Scattering* (Wiley, New York, 1976).
 [6] J.P. Munch, P. Lemarchal, and S. Candau, *J. Phys.* **38**, 1499 (1977).
 [7] G.E. Uhlenbeck and L.S. Ornstein, *Phys. Rev.* **36**, 823 (1930); J.D.G. Mc Adam, T.A. King, and A. Knox,

- Chem. Phys. Lett. **26**, 6 (1974); K.L. Wun and F.D. Carlson, *Macromolecules* **8**, 190 (1975).
- [8] P.N. Pusey and W. van Meegen, *Physics A* **157**, 705 (1989).
- [9] J.G.H. Joosten, E.T.F. Geladé, and P.N. Pusey, *Phys. Rev. A* **42**, 2161 (1990).
- [10] *Laser Speckle and Related Phenomenon*, edited by J.C. Dainty (Springer-Verlag, Berlin, 1975).
- [11] B. Chu, *Laser Light Scattering* (Academic, New York, 1974).
- [12] P. Goldbart and N. Goldenfeld, *Phys. Rev. Lett.* **58**, 2676 (1987).
- [13] R. Nossal, *J. Appl. Phys.* **50**, 3105 (1979).
- [14] S.J. Candau, F. Ilmain, F. Schosseler, and J. Basitde, *Mater. Res. Soc. Symp. Proc.* **177**, 3 (1990).
- [15] D.L. Johnson, *J. Chem. Phys.* **77**, 1531 (1982).
- [16] P.G. de Gennes, *Scaling Concepts in Polymer Physics* (Cornell University Press, Ithaca, 1979).
- [17] I. Nishio, J.C. Reina, and R. Bansil, *Phys. Rev. Lett.* **59**, 684 (1987); C. Konak, R. Bansil, and J.C. Reina, *Polymer* **31**, 2333 (1990).
- [18] J.E. Martin, J. Wilcoxon, and J. Odinek, *Phys. Rev. A* **43**, 858 (1991).
- [19] J.S. Hwang and H.Z. Cummins, *J. Chem. Phys.* **79**, 5188 (1983).
- [20] W. Brown and R. Rymden, *Macromolecules* **19**, 2924 (1986); L. Fang, W. Brown, and C. Konak, *Polymer* **31**, 1960 (1990).
- [21] E. Jakeman, C.J. Oliver, and E.R. Pike, *J. Phys. A* **3**, L45 (1970).
- [22] D.J. Pine, D.A. Weitz, G. Maret, P.E. Wolf, E. Herbolzheimer, and P.M. Chaikin, *Scattering and Localization of Classical Waves in Random Media*, edited by P. Sheng (World Scientific, Singapore, 1990).
- [23] K. Schätzel, *Quantum Opt.* **2**, 287 (1990), and references therein.

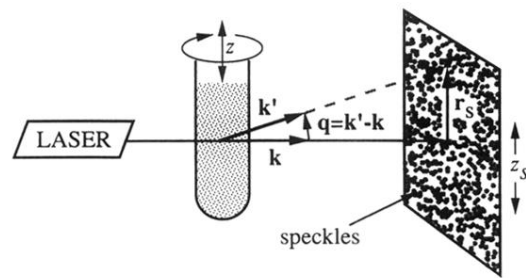


FIG. 1. Schematic geometry for a dynamic-light-scattering experiment, where we imagine that either the sample (coordinates z) or the detector (coordinates z_s) can be translated. The detector is schematically replaced by a screen to illustrate the speckle pattern.